Organic Electronics 13 (2012) 1420–1429

Contents lists available at SciVerse ScienceDirect

Organic Electronics

journal homepage: www.elsevier.com/locate/orgel

Current and Shot noise in DNA chains

J.H. Ojeda [a], M. Pacheco [b], L. Rosales [b,*], P.A. Orellana [c]

[a] GFM-Escuela de Física, Universidad Pedagógica y Tecnológica de Colombia, Tunja, Colombia
[b] Departamento de Física, Universidad Técnica Federico Santa María, Casilla 110 V, Valparaíso, Chile
[c] Departamento de Física, Universidad Católica del Norte, Casilla 1280, Antofagasta, Chile

ARTICLE INFO

Article history:
Received 26 November 2011
Received in revised form 27 February 2012
Accepted 24 March 2012
Available online 17 April 2012

Keywords:
DNA molecules
Transport
Shot noise
Fano factor

ABSTRACT

In this paper we studied the transport properties of a finite homogeneous fragments of DNA composed by N base pairs of Guanine (poly (G)) and Cytosine (poly (C)) connected to two semi-infinite leads. We study these molecules adopting different models within a nearest neighbour tight-binding approach. We proposed a semi-analytic method for the calculation of the transport properties of DNA molecules by using Green's function techniques within a real-space renormalization scheme. We studied the transmission probability, the I–V characteristics and the Noise power of current fluctuations as a function of intrasite and DNA-leads coupling parameters. Our results show different transport regimes for these molecular systems as a function of the coupling intensities, exhibiting metal–semiconductor transitions.

1. Introduction

In the last decades, there has been an increasing interest in the study of molecular electronic devices. In the literature, it is possible to find several proposed systems such as carbon nanotubes [1], organic molecules [2] and DNA molecules attached to metallic contacts [3–17]. All these systems exhibit interesting electronic behaviours useful for the development of new technological applications.

In particular, the transport properties of DNA molecules is still an interesting and controversial issue, due to the diversity of electronic behaviours reported by a variety of experimental studies. Those reports show that depending on the type and composition of the considered systems, the DNA molecules behave as superconducting [3], metal [4–8], semiconductor [9–15] or insulator [16,17].

Electronic transport in DNA molecules can be considered as discrete jumps between pairs of nucleotide bases. The two strands representing the double helix structure of DNA form two channels of propagation of the electrons [18], which can be controlled by applying gate voltages over the molecules. The current passing through these molecular systems is, in general, a non-linear function of the applied voltages. Due to this non-linear behaviour, it is possible to observe quantum fluctuations in the transport properties of DNA systems. In the absence of scattering processes, these fluctuations are known as the noise power spectrum which, in a steady state, is described by the Shot noise. The noise power provides an important information about the electronic correlation by means of the Fano factor (F), which indicates whether the magnitude of the noise reaches a Poisson ($F = 1$) or sub-poisson ($F < 1$) limits [19].

In this work we propose a semi-analytic method for the calculation of the transport properties of DNA molecules. By using a nearest neighbour tight binding Hamiltonian and based on the Green's function formalisms, we calculated the transmission probability, the I–V characteristics, the Shot noise and the Fano factor of molecules composed by homogeneous segments of pairs of basis poly (G) and poly (C), connected to two semi-infinities metallic contacts, as it is shown in Fig. 1.

To describe these molecules we have adopted the Fishbone (Fig. 1b) and the Ladder model (Fig. 1c). Both representations consider the DNA molecules as a planar

* Corresponding author.
E-mail address: luis.rosalesa@usm.cl (L. Rosales).

1566-1199/$ - see front matter © 2012 Elsevier B.V. All rights reserved.
http://dx.doi.org/10.1016/j.orgel.2012.03.036

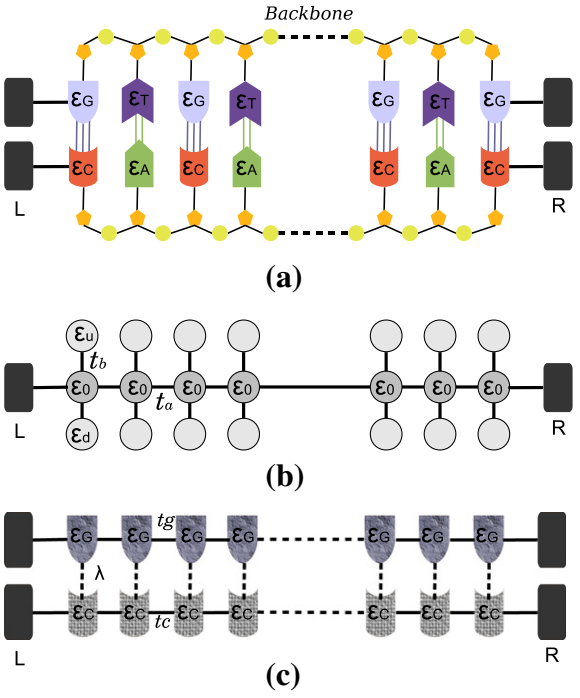

Fig. 1. (a) Flat segment of DNA molecule, (b) Fishbone model and (c) Ladder model.

structures composed by N unit cells coupling to the leads. By applying real-space renormalization techniques, we obtain one-dimensional effective models for which we analytically determined the transmission coefficients [20]. With this expression, we numerically calculate the I–V characteristics, the Shot noise and the Fano factor, reducing efficiently the computational time of calculus. We have focused our analysis in the modulations of the transport properties as a function of the intrasite and the DNA-leads coupling potentials. Our results show different electronic behaviours as a function of the coupling intensities, exhibiting transitions between metal and semiconductor regimes.

2. Formalism

We have studied the transport properties of DNA molecules by using the Landauer–Büttiker [19,21] formalism based on Green's function techniques within a real-space renormalization approach (decimation procedure) [22,23]. In this scheme, the Fishbone and Ladder DNA representations are transformed into an effective linear monoatomic chain, as it is shown in Fig. 2.

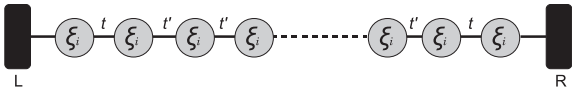

Fig. 2. Effective one-dimensional model: linear monoatomic chain of N sites connected to two metallic leads.

The Green's function of the DNA molecules coupled to the leads are calculated by using the Dyson equation $G = G^0 + G^0(\Sigma_L + \Sigma_R)G$, where G^0 is the bare Green's function of the isolated DNA molecule and Σ_L and Σ_R are the self-energies of the left and right lead, respectively.

In a general approach, the transmission probability can be obtained by using the Fischer–Lee [21] relationship, which is given by:

$$T(E) = Tr\left[\Gamma^L G^r \Gamma^R G^a\right]. \tag{1}$$

where $\Gamma^{L(R)} = i\left(\Sigma^{L(R)} - \Sigma^{L(R)\dagger}\right)$ is the spectral matrix density of the left (right) lead, which has non-null elements only for Γ^L_{11} and Γ^R_{NN}, respectively.

Due to the systems can be renormalized into an effective linear chain, the transmission probability can be written as:

$$T(E) = \Gamma^L_{11}\Gamma^R_{NN}|G^r_{1N}|^2 \tag{2}$$

where G^r_{1N} is given by:

$$G^r_{1N} = \frac{G^0_{1N}}{\left(1 - \Sigma^L G^0_{11}\right)\left(1 - \Sigma^R G^0_{NN}\right) - \Sigma^L\Sigma^R\left(G^0_{1N}\right)^2} \tag{3}$$

The Green's function G^0_{1N}, G^0_{NN} and G^0_{11} can be analytically determined by using the renormalization techniques. In our calculations we take $\Sigma^L = \Sigma^R = -i\Gamma/2$, and $G^0_{NN} = G^0_{11}$, so we can rewrite the Eq. (2) as:

$$T(E) = \frac{\frac{\Gamma^2}{4}\left(G^0_{1N}\right)^2}{\left|\left[1 + \frac{i\Gamma}{2}G^0_{NN}\right]^2 + \frac{\Gamma^2}{4}\left(G^0_{1N}\right)^2\right|^2} \tag{4}$$

The current passing through the DNA molecules can be considered as a scattering process of an electron between the leads. Using the Landauer formalism, the I–V characteristics can be obtained by the following expression [21,24]:

$$I(V) = \frac{2e}{h}\int_{-\infty}^{\infty}(f_L - f_R)T(E)dE \tag{5}$$

where $f_{L(R)}$ is the Fermi–Dirac distribution function given by $f_{L(R)} = f(E - \mu_{L(R)})$, where $\mu_{L(R)} = E_f \pm eV/2$ is the chemical potential. For simplicity we have assumed that the bias voltage drops at the DNA-lead interfaces. This assumption does not affect the qualitative behaviour of the I–V characteristics of these molecular systems.

The noise power of current fluctuations (NPCF) is calculated by the expression [19,24]:

$$S = S_0\int_{-\infty}^{\infty}[T(E)\{f_L(1 - f_L) + f_R(1 - f_R)\} + T(E)\{1 - T(E)\}(f_L - f_R)^2]dE \tag{6}$$

where $S_0 = \frac{2e^2}{\pi\hbar}$. The first two terms of this equation correspond to the equilibrium noise contribution and the last term gives the non-equilibrium or Shot noise contribution to the power spectrum. By calculating the NPCF (S), and the total current flowing through the DNA molecules, we can evaluate the Fano factor F by the following relationship [19]:

$$F = \frac{S}{2eI} \tag{7}$$

For $F = 1$, the Shot noise achieves the Poisson limit for which there is not a correlation between the charge carriers. On the other hand, for $F < 1$, the Shot noise achieves the sub-Poisson limit and it provides the information about the quantum correlation of the charge carriers [26].

2.1. Fishbone model

In the Fishbone model [25] the DNA molecules are described by N unit cells, each one composed by three atomic sites, one site corresponds to the base pair poly (G)-poly (C) and the two lateral sites correspond to the backbone formed by sugar-phosphate molecules. Due to the strong coupling between the poly (G) and poly (C) bases, this model considers the DNA molecules as a linear chain with an effective on-site energy ε_0 and an intersite coupling t_a. Each site in this monoatomic sequence is coupled to a backbone molecule by a potential t_b. The on-site energies of the backbone are labelled as ε_α, where $\alpha = u, d$ correspond to upper and lower molecules respectively, Fig. 1b.

In this model the single-band tight-binding Hamiltonian is given by $H = H_{DNA} + H_C + H_I$. The term H_{DNA} represents the DNA molecule, H_C is the lead contribution and H_I is the molecule–lead interaction, which are given by:

$$H_C = \sum_{\beta=L,R}\sum_{k_\beta} \varepsilon_{k_\beta} c^\dagger_{k_\beta} c_{k_\beta}$$

$$H_I = \sum_{k_L}\left(V_L c^\dagger_{k_L} d_1 + V^*_L d^\dagger_1 c_{k_L}\right) + \sum_{k_R}\left(V_R c^\dagger_{k_L} d_N + V^*_R d^\dagger_N c_{k_R}\right) \tag{8}$$

where $c^\dagger_{k_{L(R)}}$ is the creation operator of an electron in a state $k_{L(R)}$ and energy $\varepsilon_{k_{L(R)}}$ and $d^\dagger_i$ is the creation operator of an electron at the site i in the DNA molecule. The coupling between each lead (left and right) with the DNA is given by the term $V_{L(R)}$.

By using the decimation procedure, it is straightforward to transform H_{DNA} in a Hamiltonian corresponding to a one-dimensional chain with N sites with effective on-sites energies given by:

$$\xi_i(E) = \varepsilon_0 + \frac{t_b^2}{E-\varepsilon_u} + \frac{t_b^2}{E-\varepsilon_d}. \tag{9}$$

With this consideration, the effective Hamiltonian of the DNA molecule can be written as:

$$H_{ADN} = t_a \sum_i \left(d^\dagger_i d_{(i+1)} + d^\dagger_{(i+1)} d_i\right) + \sum_i \xi_i(E) d^\dagger_i d_i, \tag{10}$$

where $t_a = t = t'$ is the coupling between sites of the new effective chain, Fig. 2.

In order to obtain the transmission probability of Eq. (4) we must calculate the matrix element G^r_{1N}. By using the Dyson equation it can be shown [27] that:

$$G^r_{1N}(E) = \frac{G^{r0}_{1N}}{\left(1-\Sigma^L G^{r0}_{11}\right)\left(1-\Sigma^R G^{r0}_{NN}\right) - \Sigma^L\Sigma^R\left(G^{r0}_{1N}\right)^2}.$$

The bare Green's function elements of the DNA molecule $\left[G^{r0}(E)\right]_{ij}$ can be analytically calculated. For brevity we quote only the matrix elements G^{r0}_{1N}, G^{r0}_{11} and G^{r0}_{NN}:

$$G^{r0}_{1N}(E) = (U_N(x) t_a)^{-1}, \tag{11}$$

$$G^{r0}_{11}(E) = G^{r0}_{NN}(E) = t_a^{-1}\frac{U_{N-1}(x)}{U_N(x)} \tag{12}$$

where the $U_N(x)$ are the generalized Chebyshev polynomials that satisfy the recurrence relation $U_{N+1}(x) = 2xU_N(x) - U_{N-1}(x)$, with $U_0 = 1$ and $U_1 = 2x$. Here $x = 1/2g_0t_a$ with:

$$g_0 = \frac{(E-\varepsilon_u)(E-\varepsilon_d)}{(E-\varepsilon_0)\left[(E-\varepsilon_u)(E-\varepsilon_d) - 2t_b^2\right]}, \tag{13}$$

and $\varepsilon_0 = (\varepsilon_u + \varepsilon_d)/2$.

The transmission probability can be written in a compact form as,

$$T(E) = \frac{\Gamma^2 t_a^2 [U_N]^2}{\left[t_a^2 U_N^2 - \frac{\Gamma^2}{4}U^2_{N-1} + \frac{\Gamma^2}{4}\right]^2 + [\Gamma t_a U_N U_{N-1}]^2} \tag{14}$$

where $\Gamma = \Gamma^L_{11} = \Gamma^R_{NN}$.

If $|x| \leqslant 1$, $U_N = \sin[(N+1)\vartheta]/\sin\vartheta$ with $\vartheta = \cos^{-1}(x)$ and if $|x| > 1$, $U_N = \sinh[(N+1)\xi]/\sinh\xi$ with $\xi = \cosh^{-1}$ z(x).

By making a simple analysis on the above equation we can observe that if $\xi \to \infty$ then $T(E) \to 0$ as $T(E) \propto e^{-N\xi}$. With this expression for the transmission probability, we calculate the I–V characteristics, the Shot noise and the Fano factor of DNA molecules within this model.

2.2. Ladder model

In this model, the DNA molecules are described by two linear atomic chains (*up* and *down*) composed of N sites, laterally coupled between each other by an intrasite potential λ. These chains represent the poly (G) and poly (C) bases of the DNA, respectively. The intersite potential for the poly (G) chain is taken as $t_g = t_u$, whereas for the poly (C) chain is taken as $t_c = t_d$. The onsite energies for each linear chain are considered by $\varepsilon_G = \varepsilon_u$ and $\varepsilon_C = \varepsilon_d$. In this description of the DNA, the backbone molecules are taken into account implicitly within the onsite energies terms for each base.

With the above considerations, the full system is described by a tight-binding Hamiltonian given by $H = H_{DNA} + H_L + H_I$, with:

$$H_{DNA} = \sum_{i,\alpha=u,d} t_\alpha\left(a^{\alpha\dagger}_i a^\alpha_{(i+1)} + a^{\alpha\dagger}_{(i+1)} a^\alpha_i\right) + \sum_{\alpha=u,d}\varepsilon_\alpha a^{\alpha\dagger}_i a^\alpha_i + \lambda\sum_i\left(a^{u\dagger}_i a^d_i + a^{d\dagger}_i a^u_i\right) \tag{15}$$

$$H_L = \sum_{k_L}\varepsilon_{k_L} c^\dagger_{k_L} c_{k_L} + \sum_{k_R}\varepsilon_{k_R} c^\dagger_{k_R} c_{k_R} \tag{16}$$

$$H_I = \sum_{k_L,\alpha=u,d}\left(T_L c^{\alpha\dagger}_{k_L} a^\alpha_1 + T^*_L a^{\alpha\dagger}_1 a^\alpha_1\right) + \sum_{k_R,\alpha=u,d}\left(T_R c^{\alpha\dagger}_{k_R} a^\alpha_N + T^*_R a^{\alpha\dagger}_N c_{k_R}\right) \tag{17}$$

where $a^{\alpha\dagger}_i$ is the creation operator of an electron at site i corresponding to the $\alpha = u, d$ base, ε_α is the onsite energy of the α base, the operator $c^\dagger_{k_{L(R)}}$ is the creation operator of

an electron in a state $k_{L(R)}$ and energy $\varepsilon_{k_{L(R)}}$ and $T_{L(R)}$ is the coupling between each lead with the DNA molecule.

By using the decimation procedure, we can transform the ladder representation into an effective one-dimensional chain of sites, obtaining renormalized local Green's functions and effective intersite couplings which contain all the information of the planar DNA molecule. In order to obtain the transmission probability given by Eq. (4), we determine the Green's functions G^{r0}_{1N}, G^{r0}_{11} and G^{r0}_{NN} of the effective linear chain.

The following equations for each G_{iN} are obtained (see Appendix for the complete deduction of these expressions):

$$G_{1N} = \frac{y^2 \widetilde{t_d}(-1)^{N-1}}{2xD_{N-1} - aD_{N-2}} \tag{18}$$

$$G_{NN} = \frac{yD_{N-1}}{2xD_{N-1} - aD_{N-2}} \tag{19}$$

where

$$D_j = 2xD_{j-1} - D_{j-2} \tag{20}$$

for $j \geqslant 3$ and with the initial conditions:

$$D_1 = 2x$$
$$D_2 = 4x^2 - a \tag{21}$$

with

$$2x = \frac{1}{\widehat{g^d_0}\widehat{t_d}}; \quad a = \frac{\widetilde{g^d_0}\widetilde{t_d}}{\widehat{g^d_0}\widehat{t_d}} \qquad y = \frac{\widetilde{g^d_0}}{\widehat{g^d_0}\widehat{t_d}} \tag{22}$$

Here, $\widehat{g^d_0}, \widehat{t_d}, \widetilde{g^d_0}$ and $\widetilde{t_d}$ are the renormalized Green's function and intersite potential for the *down* chain. The same expressions can be obtained for the *up* chain.

By calculating recursively the above expressions, we can determine semi-analytically the transmission probability for an electron passing through the DNA molecule. By using these results we numerically calculate the I–V characteristic, the Shot noise and the Fano factor of the considered systems. These results are shown further in this paper.

3. Results

3.1. Fishbone model

Results of the transmission coefficient as a function of the energy, for a system composed by $N = 10$ pairs of bases and for different values of intrasite coupling t_b, are displayed in the upper panel of Fig. 3. In order to compare with experimental measures [9] of homogeneous chains of poly (G) and poly (C), we have taken the DNA-leads coupling $\Gamma = t_a$, the temperature $T = 0$ K, the intersite potential $t_a = 0.54$ eV and the onsite energies by $\varepsilon_0 = \varepsilon_u = \varepsilon_d = 0$.

By using the analytic results given by Eq. (14) it is easy to understand the results for the transmission probability. The gap of the transmission can be determined by analysing the limit $|x| = 1$ in the argument of the Chebyshev polynomials. This equation gives four energy values which define two bands and a gap region where the transmission is null. The values of these energies are:

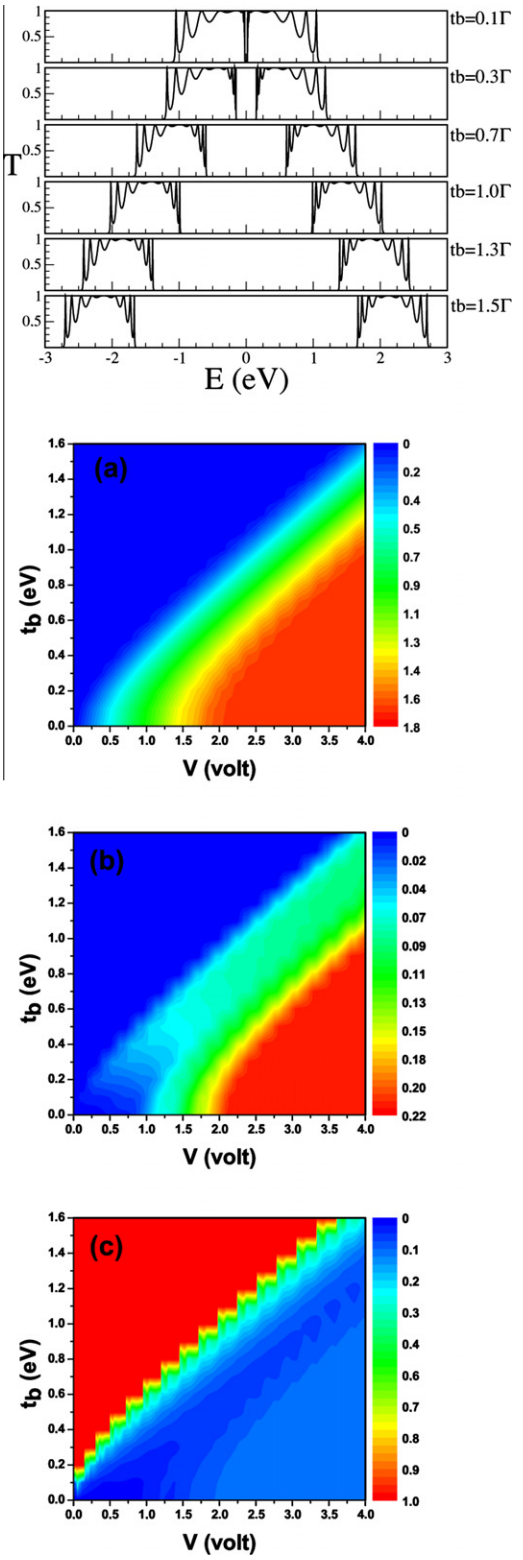

Fig. 3. Upper panel: Transmission probability for different values of intrasite coupling t_b, for $\Gamma = t_a$, temperature $T = 0$ K, $t_a = 0.54$ eV, $N = 10$. Contour plots: (a) I–V characteristic I/I_0, (b) Shot noise S/S_0 and (c) Fano factor F as a function of bias voltage and intrasite coupling potential t_b, for the same parameters.

$$E_1 = -t_a - t_a\sqrt{1+2(t_b/t_a)}$$
$$E_2 = t_a - t_a\sqrt{1+2(t_b/t_a)}$$
$$E_3 = -t_a + t_a\sqrt{1+2(t_b/t_a)}$$
$$E_4 = t_a + t_a\sqrt{1+2(t_b/t_a)} \quad (23)$$

The transmission spectrum presents two symmetric bands of width $W = 2t_a$, exhibiting a finite number of unitary peaks at some defined energies. These energy values can be obtained by solving the transcendental equation $T(E) = 1$, with $T(E)$ given by Eq. (14). The bands are separated by a gap of width

$$\Delta = 2t_a\left[\sqrt{1+2\left(\frac{t_b}{t_a}\right)^2}-1\right]$$

that depends of both the intrasite and intersite coupling parameters. This result indicates that the DNA molecules could behave as a semiconductor or metal depending on these coupling potentials, in accordance with results previously reported [25]. There are two regions determined by the ratio t_b/t_a, for $t_b/t_a \ll 1$ the gap has a quadratic dependence of t_b, when this coupling is increased and $t_b/t_a \gg 1$, gap shows a linear dependence with the intrasite coupling. In this plot it is possible to observe the behaviour of the gap width with the intrasite potential t_b.

The same parameter dependence is reflected in the I–V characteristic, the Shot noise and Fano factor, as it can be seen in the corresponding (a), (b) and (c) contour plots of Fig. 3. The t_b dependence of the gap width is clearly exhibited in the I–V characteristic and the Shot noise curves. Nevertheless, there is a notorious difference between these two transport properties due to the oscillations exhibited by the Shot noise in a determined range of parameters. This behaviour is produced due to the quantum fluctuations of the current as a function of the bias voltage, which are mainly determined by the quantum correlation between the electrons within the molecules. For a better analysis of this fact, we have calculated the Fano factor F, which indicates the presence (or not) of a correlation between the carriers in the systems. It is well known that for $F = 1$ the Shot noise presents a Poissonian regime and, as a consequence, there is not correlation between electrons into the DNA molecule. This happens for zero current and for a certain range of values of intrasite hopping t_b and bias voltage V. On the other hand, for $F < 1$, the Shot noise presents a sub-Poissonian limit and it is expected non-null quantum carrier correlations. This happens when the current increases as a function of the bias voltage V, for different values of the intrasite potential t_b.

In what follow we analyse the effect of the DNA-lead coupling on the transport properties of DNA molecules. Theoretical results about contact-dependent effects and tunneling currents through DNA molecules have been reported before by Macia et al. [28], they demonstrates the importance of contact effects on turn-on currents characteristics. Results of the transmission probability as a function of the Fermi energy, for a system composed by $N = 10$ pairs of bases poly (G) and poly (C) and for different values of the DNA-lead coupling Γ, are displayed in the upper panel of Fig. 4. In order to compare with experimental measurement [9], we have fixed the couplings $t_a = 0.54$ eV and $t_b = 0.75$ eV and the onsite energies $\varepsilon_0 = \varepsilon_u = \varepsilon_d = 0$ with the temperature $T = 0$ K.

The probability of transmission shows a strong dependence on the DNA-lead coupling strength, for $\Gamma \ll t_a$ the chain is weakly linked to the leads and a series of N well defined transmission resonances of unit height appear. This is a regime of resonant tunnelling where the resonances correspond to the energies of the quasi-bound electronic states confined in a molecular wire of N atomic sites. For strong coupling $\Gamma \gg t_a$ the electronic structure is modified significantly, which leads to resonances shifted and broadened and not related to the isolated molecular levels. In this strong coupling regime the number of resonances is $N-2$, indicating the hybridization between the end sites of the chain and the leads. For the critical value $\Gamma = t_a$ the transmission is maximum for all energies within the side bands.

Contour plots in Fig. 4 show current–voltage characteristics I/I_0, Shot noise S/S_0 and Fano factor F as a function of the lead-DNA coupling strength Γ and the bias voltage. We note that the maximum current amplitude occurs around the critical value of $\Gamma = t_a$, for which the mean value of the transmission is maximum within the band. On the other hand, the contour plot for S/S_0 shows two areas where the noise power of the current fluctuation is large. These areas correspond to values of Γ for which the DNA-lead coupling is either weak or strong. This can be explained by considering the mean value of the Shot noise at temperature $T = 0$, per energy range ΔE equal to the bandwidth W. With this consideration, $S = \overline{T}(1-\overline{T})\Delta E$ will be maximum if $dS/d\overline{T} = (1-\overline{T})\Delta E - \overline{T}\Delta E = 0$, and therefore $S_{\max}$ is found when $\overline{T} = 1/2$. The Shot noise goes from the Poisson limit ($F = 1$) to the sub-Poisson limit ($F < 1$) as long as we cross the threshold voltage determined by the transmission gap. This emphasizes that the electrons are correlated after the tunnelling process has occurred. We also observe an area for coupling values around $\Gamma = t_a$, where the Fano factor and the noise power of the current fluctuations reaches minimum values. For these values the electronic correlation will be maximum.

In Fig. 5 we show the behaviour of the current (I), the Shot noise (S) and Fano factor (F) as a function of the molecule length. For $T = 0$ K and $\Gamma = 0.025$ eV it is observed that the current shows staircase-like structure as a function of the applied bias voltage. This is due to the sharp resonances those appear in the transmission spectrum in this weak DNA-lead coupling limit. The number of steps is equal to the number of atomic sites considered. As the number of poly (G) and poly (C) base-pairs in the chain is increased, the transport properties that we have been discussing are not affected.

3.2. Ladder model

Results of the transmission probability as a function of the Fermi energy, for a system composed by $N = 10$ pairs of bases poly (G) and poly (C) and for different values of the intrasite coupling λ, are displayed in the upper panel of Fig. 6. In order to reproduce experimental measurements, in this model we have taken the temperature $T = 0$ K, the

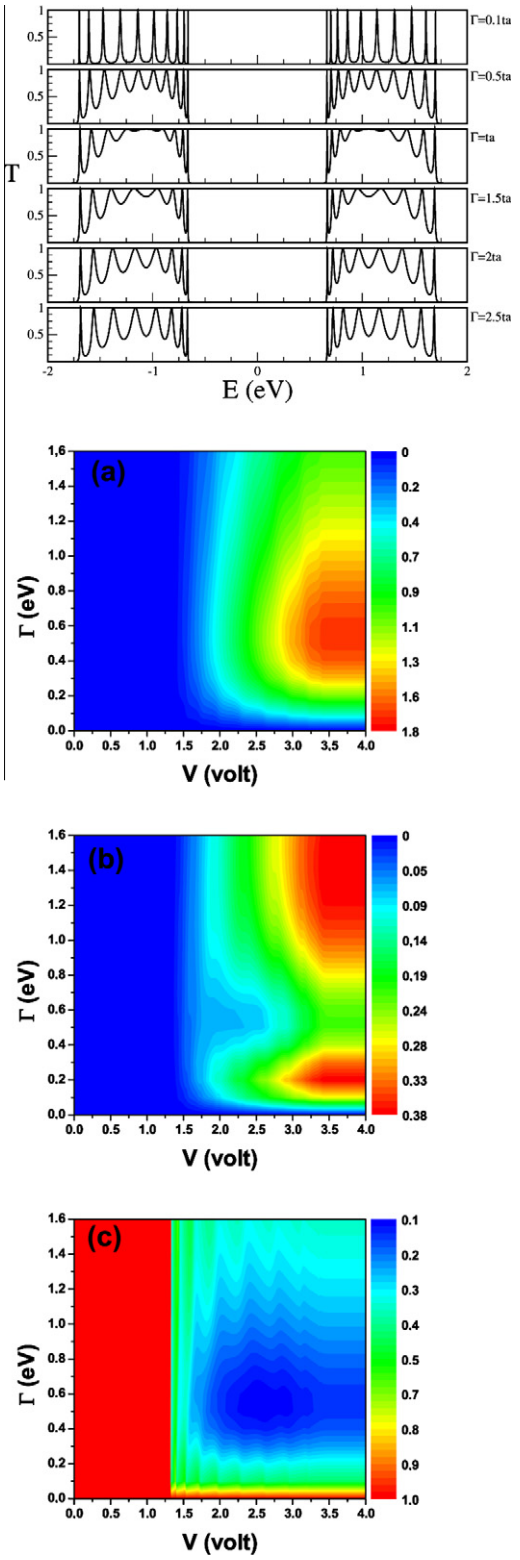

Fig. 4. Upper panel: transmission probability for different values of the lead-DNA coupling strength Γ for a $N = 10$ DNA molecule with fixed values of hopping parameters $t_a = 0.54$ eV, $t_b = 0.75$ eV and $T = 0$ K. Contour plots: (a) I–V characteristic I/I_0, (b) Shot noise S/S_0 and (c) Fano factor F as a function of Γ and the bias voltage.

onsite energies $\varepsilon_g = 1.14$ eV, $\varepsilon_c = -1.06$ eV and the intersite potential $t_c = t_g = \tau = 0.27$ eV [9,29–32].

It is possible to observe that the amplitude of the transmission probability changes as the intrasite coupling λ is increased. This behaviour can be explained by examining the effective one dimensional chain obtained after the decimation procedure, where the renormalized intersite coupling and the renormalized local Green's functions depend on the coupling λ (see Appendix), and therefore, it affects the total transmission of the electrons through the system.

On the other hand, our results exhibit a non-linear gap-width dependence on the intrasite coupling λ. In order to explain this behaviour, we can describe the system by using an effective model formed by two linear chains of sites (*up* and *down*) interconnected between each other by a coupling λ, and connected to two leads by a coupling Γ. We have considered an intersite coupling potential equal to τ, as is it shown in Fig. 2.

It is possible to decouple these two chains by using a base of wavefunctions which allows us to diagonalize the Hamiltonian of the isolate DNA molecule. We obtain two independent effective linear chains, with onsite energies given by:

$$\varepsilon_{\pm} = \frac{(\varepsilon_d + \varepsilon_u)}{2} \pm \frac{1}{2}\sqrt{(\varepsilon_d - \varepsilon_u)^2 + 4\lambda^2} \tag{24}$$

where these two energies $\varepsilon_{\pm}$ correspond to the center of each band of the transmission probability of Fig. 6.

Within this effective model, it is expected that electrons can propagate into the system as plane waves of the form: $\Psi_j = \alpha_{\pm} e^{i\kappa_{\pm} j} + \beta_{\pm} e^{-i\kappa_{\pm} j}$, where $\kappa_{\pm}$ are taken as normalized wavevectors, and $\alpha_{\pm}$ and $\beta_{\pm}$ are amplitudes of probability. In the tight-binding approximation, the energy dispersion relationship of these chains can be considered by: $\varepsilon - \varepsilon_{\pm} = 2\tau \cos\kappa_{\pm}$. The band edges are determined by the condition: $|\ (\varepsilon - \varepsilon_{\pm})/2\tau\ | = 1$, which gives us the following set of solutions:

$$\begin{aligned} E_1 &= \varepsilon_+ + 2\tau \\ E_2 &= \varepsilon_+ - 2\tau \\ E_3 &= \varepsilon_- + 2\tau \\ E_4 &= \varepsilon_- - 2\tau \end{aligned} \tag{25}$$

By using these expressions, we can determine the width of the two bands in the transmission probability. By taking the differences $E_1 - E_2$ and $E_3 - E_4$ we obtain the bandwidth $W = 4\tau$ in concordance with results of previous reports [33,25]. The gap of the transmission is obtained by taking the difference $E_2 - E_3$, which shows a dependence on the intrasite coupling λ given by the expression:

$$\Delta = E_2 - E_3 = \sqrt{(\varepsilon_u - \varepsilon_d)^2 + 4\lambda^2} - 4\tau \tag{26}$$

From the above expression, it is clear that for $\lambda = 0$ the gap still has a non-null value: $\Delta = |\ \varepsilon_u - \varepsilon_d\ | - 4\tau$.

The gap behaviour of the transmission probability as a function of the coupling λ is reflected in the I–V characteristic, the Shot noise and the Fano factor, as it is shown in the corresponding (a), (b) and (c) contour plots of Fig. 6. By analysing the limits of the Eq. (26), it is possible to understand the

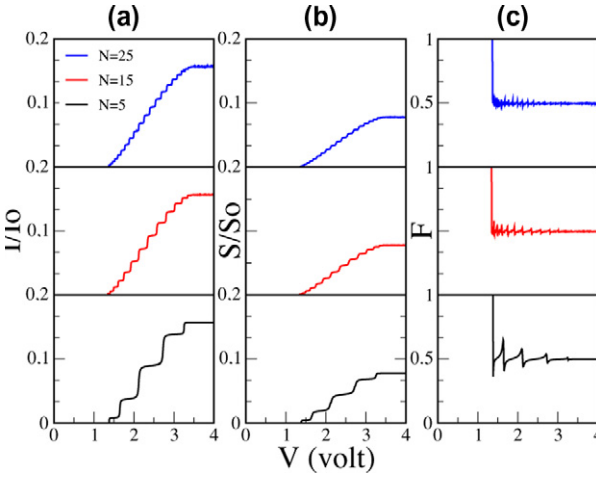

Fig. 5. (a) I–V characteristics I/I_0, (b) Shot noise S/S_0 and (c) Fano factor F, for different molecule lengths. The hopping parameters are $t_a = 0.54$ eV, $t_b = 0.75$ eV and DNA-lead coupling $\Gamma = 0.025$ eV for $T = 0$ K.

gap of these transport properties. For $\lambda \ll (\varepsilon_u - \varepsilon_d)$ the gap is $\Delta \simeq \{|(\varepsilon_u - \varepsilon_d)| \, [1 + 2\lambda^2/(\varepsilon_u - \varepsilon_d)^2] - 4\tau\}$, indicating a quadratic dependence with λ, whereas for $\lambda \gg |\varepsilon_u - \varepsilon_d|$ the gap is $\Delta \simeq 2\lambda - 4\tau$, indicating a linear evolution as a function of the intrasite coupling.

On the other hand, in the contour plot for the current–voltage characteristics I/I_0 we note that the maximum current amplitude occurs in the range of λ between 0.1 eV and 0.5 eV, for which the transmission probability is maximum within the bands. The contour plot for the Shot noise S/S_0 shows a region where the noise power is large, corresponding to values of λ between 0.8 eV and 1.3 eV approximately. As we have discussed before in the Fishbone model, $S_{\max}$ occurs when $\overline{T} = 1/2$. The Shot noise goes from the Poisson limit ($F = 1$) to the sub-Poisson limit ($F < 1$) as long as we cross the threshold voltage determined by the transmission gap. This again emphasizes the correlation between electrons after the tunnelling process has occurred.

In what follows, we analyse the same molecule but now considering the intrasite coupling λ constant and modifying the DNA-leads coupling Γ. Results of the transmission probability as a function of the Fermi energy are exhibit in the upper panel of Fig. 7. It is possible to observe that the gap and the bandwidth of the transmission probability remain constant as Γ is increased. This can be seen in the expressions given by Eqs. (25) and (26).

The amplitude and the number of resonances in the transmission curves vary as the coupling Γ is modified. In the limit of weak DNA-leads coupling, $\Gamma < \tau$, the system is in a resonant tunnelling regime and therefore there are N unitary transmission peaks, one for each nucleus base in the considered molecule. On the other hand, for $\Gamma \geqslant \tau$ there is a strong coupling between the DNA molecule and the leads with the corresponding hybridization of the end sites of the molecule and the continuum of energies in the leads. As a consequence of this strong coupling, the molecular states are broadened and only $N - 2$ resonances in the transmission curves are obtained [34,35].

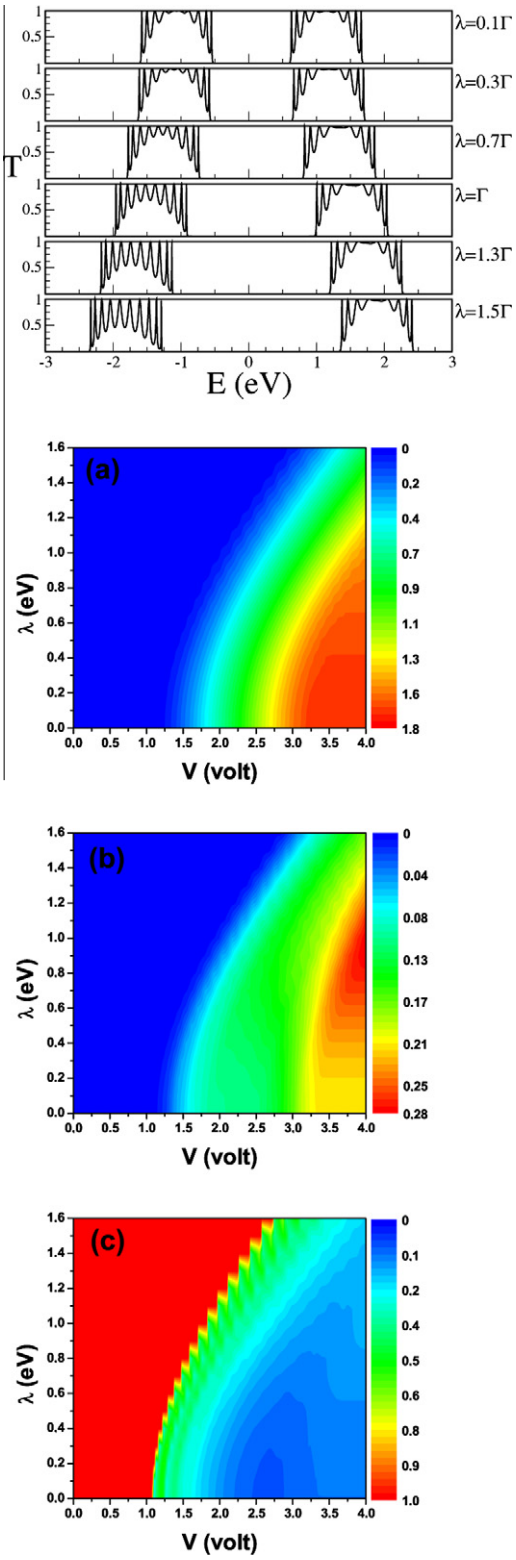

Fig. 6. Upper panel: transmission probability for different values of intrasite coupling λ, for $t_g = t_c = \tau = 0.27$ eV, $T = 0$ K, $\Gamma = \tau$, $N = 10$. Contour plots: (a) I–V characteristic I/I_0, (b) Shot noise S/S_0 and (c) Fano factor F as a function of bias voltage and intrasite coupling potential λ.

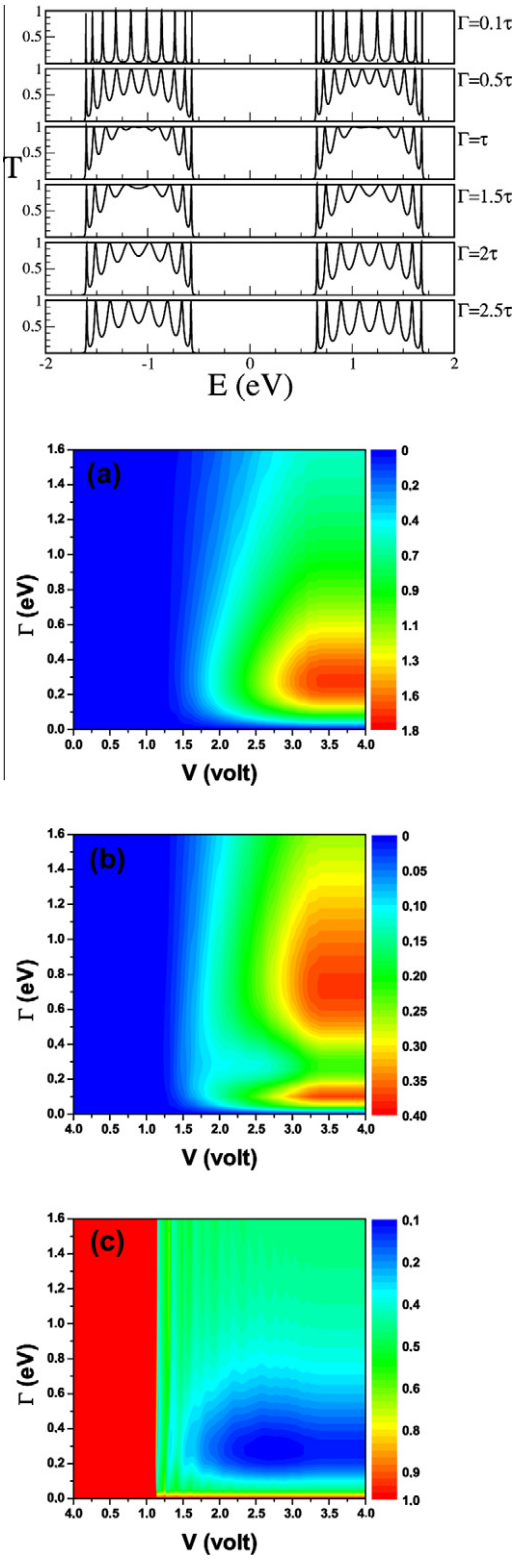

Fig. 7. Upper panel: transmission probability for different values of DNA-leads coupling $\Gamma, t_g = t_c = \tau = 0.27$ eV, $\lambda = 0.25$ eV, $T = 0$ K and $N = 10$ atomic sites. Contour plots: (a) I–V Characteristics I/I_0, (b) Shot noise S/S_0 and (c) Factor Fano F as a function of bias voltage and DNA-leads coupling Γ.

Contour plots in Fig. 7 show (a) current–voltage characteristics I/I_0, (b) Shot noise S/S_0 and (c) Fano factor F as a function of the lead-DNA coupling strength Γ and the bias voltage. In the Fig. 7a, it is observed a maximum amplitude in the I–V characteristics when the DNA-leads coupling reach the critical value $\Gamma = \tau$. The contour plot of the Shot noise presents two areas where the Noise power is large. These areas correspond to values of Γ between 0.1 eV − 0.15 eV and 0.6 eV − 1 eV for which the mean value of the transmission probability, as we discuss before, is $\overline{T} = 1/2$. This is reflected in the Fano factor, where it is possible to observe a lower carrier correlation in the same range of values of Γ.

In summary in this paper we have proposed a semi-analytic method for the calculation of the transport properties of homogeneous DNA molecules. We have studied these molecules by adopting two different models: Fishbone and Ladder models, within a nearest neighbour tight-binding approach. By using Green's function techniques within a real-space renormalization scheme, we have calculated the transmission probability, the I–V characteristics, the noise power of current fluctuations and Fano factor of a finite fragment of DNA composed by N base pairs of Guanine (poly (G)) and Cytosine (poly (C)) connected to two semi-infinite leads. These properties have been studied as a function of intrasite and DNA-leads coupling parameters in both models. Our results show different transport regimes for these molecular systems as a function of the coupling intensities, exhibiting metal–semiconductor transitions in good agreement with experimental results [9].

The authors acknowledge to Dr. F. Domínguez-Adame for a helpful discussions. This work was financial supported by USM Internal Grant No. 110971, FONDECYT Program, Grants Nos. 11090212, 1100560 and 1100672, and DIN-UPTC.

Appendix A. Green's function G_{1N} for Ladder model

The decimation procedure is started by writing the local Green's functions for each chain by:

$$g_0^d = \frac{1}{E - \varepsilon_d}$$
$$g_0^u = \frac{1}{E - \varepsilon_u} \tag{A.1}$$

where d, u represent *down* and *up* chain respectively. According to the ladder model, the Green's functions G_{ij} for the first sites of both chains (labeled by 0) are given by:

$$G_{00}^d = g_0^d + g_0^d t_d G_{10}^d + g_0^d \lambda G_{00}^u$$

$$G_{00}^u = g_0^u + g_0^u t_u G_{10}^u + g_0^u \lambda G_{00}^d \tag{A.2}$$

Similar expressions can be obtained for the Green's functions $G_{11}^d, G_{11}^u, G_{22}^d, G_{22}^u$, etc. By decoupling the above equations, it is possible to determine the effective local Green's function and its corresponding effective inter-site coupling. The resulting Green's functions and effective potential for the end sites are given by:

$$\widehat{g_0^d} = g_0^d \left\{ \frac{1 - \left(g_0^u t_u\right)^2 + \lambda g_0^u}{1 - \left(g_0^u t_u\right)^2 - g_0^d g_0^u \lambda^2} \right\}$$
$$t = \widehat{t_d} = \frac{t_d - t_d \left(g_0^u t_u\right)^2 + t_u \lambda^2 \left(g_0^u\right)^2}{1 - \left(g_0^u t_u\right)^2 + \lambda g_0^u} \tag{A.3}$$

and for inner sites of the down chain they are given by:

$$\widehat{g_0^d} = g_0^d \left\{ \frac{1 - 2\left(g_0^u t_u\right)^2 + \lambda g_0^u}{1 - 2\left(g_0^u t_u\right)^2 - g_0^d g_0^u \lambda^2} \right\}$$
$$t' = \widehat{t_d} = \frac{t_d\left(1 - 2(g_0^u t_u)^2\right) + (\lambda g_0^u)^2 t_u}{1 - 2\left(g_0^u t_u\right)^2 + \lambda g_0^u} \tag{A.4}$$

For the upper chain, the renormalized Green's functions are given by:

$$\widehat{g_0^u} = g_0^u \left\{ \frac{1 - \left(g_0^d t_d\right)^2 + \lambda g_0^d}{1 - \left(g_0^d t_d\right)^2 - g_0^u g_0^d \lambda^2} \right\}$$
$$t = \widehat{t_u} = \frac{t_u - t_u \left(g_0^d t_u\right)^2 + t_d \lambda^2 \left(g_0^d\right)^2}{1 - \left(g_0^d t_d\right)^2 + \lambda g_0^d} \tag{A.5}$$

and for inner sites of the upper chain:

$$\widehat{g_0^u} = g_0^u \left\{ \frac{1 - 2\left(g_0^d t_d\right)^2 + \lambda g_0^d}{1 - 2\left(g_0^d t_d\right)^2 - g_0^u g_0^d \lambda^2} \right\}$$
$$t' = \widehat{t_u} = \frac{t_u\left(1 - 2(g_0^d t_d)^2\right) + (\lambda g_0^d)^2 t_d}{1 - 2\left(g_0^d t_d\right)^2 + \lambda g_0^d} \tag{A.6}$$

With the above expressions we determine the Green's function G_{1N} of the system. We have renamed $g_0^d = \widehat{g_0^d}$ and $\widetilde{t_d} = \widehat{t_d}$ for the end sites of the chain. Then, we write a set of equations for G_{iN} with $i = 1, N$ (N the total number of atomic sites), given by:

$$\begin{aligned}
G_{1N} &= \widetilde{g_0^d}\,\widetilde{t_d} G_{2N} \\
G_{2N} &= \widehat{g_0^d}\,\widehat{t_d} G_{1N} + \widehat{g_0^d}\,\widehat{t_d} G_{3N} \\
G_{3N} &= \widehat{g_0^d}\,\widehat{t_d} G_{2N} + \widehat{g_0^d}\,\widehat{t_d} G_{4N} \\
G_{4N} &= \widehat{g_0^d}\,\widehat{t_d} G_{3N} + \widehat{g_0^d}\,\widehat{t_d} G_{5N} \\
&\vdots \qquad\qquad\qquad \vdots \\
G_{NN} &= \widetilde{g_0^d} + \widetilde{g_0^d}\,\widetilde{t_d} G_{N-1,N}
\end{aligned} \tag{A.7}$$

Rewriting the Eq. (A.7) we obtain:

$$\begin{aligned}
&2xG_{1N} - aG_{2N} = 0 \\
&2xG_{2N} - G_{1N} - G_{3N} = 0 \\
&2xG_{3N} - G_{2N} - G_{4N} = 0 \\
&2xG_{4N} - G_{3N} - G_{5N} = 0 \\
&\qquad\vdots \qquad\qquad\qquad \vdots \\
&2xG_{NN} - at_d G_{N-1,N} = y
\end{aligned} \tag{A.8}$$

where

$$2x = \frac{1}{\widehat{g_0^d}\,\widehat{t_d}}; \quad a = \frac{\widetilde{g_0^d}\,\widetilde{t_d}}{\widehat{g_0^d}\,\widehat{t_d}} \quad \text{and} \quad y = \frac{\widetilde{g_0^d}}{\widehat{g_0^d}\,\widehat{t_d}}$$

Now, we take the Eq. (A.8) to calculate each term G_{iN}, and we obtain:

$$G_{1N} = \frac{y^2 \widetilde{t_d} (-1)^{N-1}}{2xD_{N-1} - aD_{N-2}} \tag{A.9}$$

$$G_{NN} = \frac{yD_{N-1}}{2xD_{N-1} - aD_{N-2}}$$

where

$$D_j = 2xD_{j-1} - D_{j-2}$$

For $j \geqslant 3$ and with the initial conditions:

$$D_1 = 2x$$
$$D_2 = 4x^2 - a$$

By using these equations we calculate semi-analytically the transmission probability of an electron passing through the DNA molecule.

References

[1] C. Dekker, Physics Today 52 (1999) 22.
[2] S.F. Nelson, Y.Y. Lin, D.J. Gundlach, T.N. Jackson, Appl. Phys. Lett. 72 (1998) 1854.
[3] A.Yu. Kasumov, M. Kociak, S. Guron, B. Reulet, V.T. Volkov, D.V. Klinov, H. Bouchiat, Science 280 (2001) 291.
[4] O. Legrand, D. Côte, U. Bockelmann, Phys. Rev. E 73 (2006) 031925.
[5] L. Cai, H. Tabata, T. Kawai, Nanotechnology 12 (2001) 211.
[6] Y. Okahata, T. Kobayashi, K. Tanaka, M.J. Shimomura, J. Am. Chem. Soc. 120 (1998) 6165.
[7] H.W. Fink, C. Schonenberger, Nature 398 (1999) 407.
[8] A. Rakitin, P. Aich, C. Papadopouls, Yu. Kobzar, A.S. Vedeneev, J.S. Lee, J.M. Xu, Phys. Rev. Lett. 86 (2001) 3670.
[9] D. Porath, A. Bezryadin, S. de Vries, C. Dekker, Nature 403 (2000) 635.
[10] H. Cohen, C. Nogues, R. Naaman, D. Porath, Proc. Natl. Acad. Sci. USA 102 (2005) 11589.
[11] K.-H. Yoo, D.H. Ha, J.-O. Lee, J. Kim, J.J. Kim, H.-Y. Lee, T. Kawai, H.Y. Choi, Phys. Rev. Lett. 87 (2001) 198102.
[12] J.S. Hwang, K.J. Kong, D. Ahn, G.S. Lee, D.j. Ahn, S.W. Hwang, Appl. Phys. Lett. 81 (2002) 1134.
[13] B. Xu, P. Zhang, X. Li, N. Tao, Nano Lett. 4 (2004) 1105.
[14] E. Díaz, A.v. Malyshev, F. Domínguez-Adame, Phys. Rev. B 76 (2007) 205117.
[15] S. Roy, H. Vedala, A. Datta Roy, D.-H. Kim, M. Doud, K. Mathee, H.-K. Shin, N. Shimamoto, V. Prasad, W. Choi, Nano Lett. 8 (2008) 26.
[16] E. Braun, Y. Eichen, U. Sivan, G. Ben-Yoseph, Nature 391 (1998) 775.
[17] A.J. Storm, J. van Noort, S. de Vries, C. Dekker, Appl. Phys. Lett. 79 (2001) 3881.
[18] V.M.K. Bagci, A.A. Krokhin, Chaos, Solitons and Fractals 34 (2007) 104.
[19] Y.M. Blanter, M. Büttiker, Phys. Rep. 1 (2000) 336.
[20] S. Roche, Phys. Rev. Lett. 91 (2003) 108101.
[21] S. Datta, Electronic Transport in Mesoscopic Systems, Cambridge University Press, Cambridge, 1997.
[22] L. Rosales, M. Pacheco, Z. Barticevic, A. Latgé, P. Orellana, Nanotechnology 19 (2008) 065402;
L. Rosales, M. Pacheco, Z. Barticevic, A. Latgé, P. Orellana, Nanotechnology 20 (2009) 095705.
[23] M. Nardelli, Phys. Rev. B 60 (1999) 7828.
[24] S.K. Maiti, Int. J. Quant. Chem. 108(1) (2008) 135–141.
[25] G. Cuniberti, L. Graco, D. Porath, C. Dekker, Phys. Rev. B. 65 (2002) 241314.
[26] S.K. Maiti, Organic Electronics 8 (2007) 573.
[27] J.H. Ojeda, M. Pacheco, P.A. Orellana, Nanotechnology 20 (2009) 434013.
[28] E. Macia, F. Triozon, S. Roche, Phys. Rev. B 71 (2005) 113106;
E. Macia, S. Roche, Nanotechnology 17 (2006) 3002;
S. Roche, E. Macia, Mod. Phys. Lett. B 18 (2004) 847.
[29] H. Mehrez, M.P. Anantram, Phys. Rev. B 71 (2005) 115405.

[30] A.V. Malyshev, E. Díaz, F. Domínguez-Adame, J. Phys. Condens. Matter 21 (2009) 335105.
[31] A.V. Malyshev, Phys. Rev. Lett. 98 (2007) 096801.
[32] Juyeon Yi, Phys. Rev. B 68 (2003) 193103.
[33] Ai-Min Guo, Shi-Jie Xiong, Phys. Lett. A 372 (2008) 3259.
[34] Yu Zhu, Chao-Cheng Kaun, Hong Guo, Phys. Rev. B 69 (2004) 245112.
[35] S.K. Maiti, Solid State Communications 142 (2007) 398.